

# CIDEP Effects of Intramolecular Quenching of Singlet and Triplet Excited States by Nitroxide Radicals in Oligopeptides: A Potentially Useful New Method for Investigating Peptide Secondary Structures in Solution

Carlo Corvaja,<sup>\*[a]</sup> Elena Sartori,<sup>[a]</sup> Antonio Toffoletti,<sup>[a]</sup> Fernando Formaggio,<sup>[b]</sup> Marco Crisma,<sup>[b]</sup> Claudio Toniolo,<sup>\*[b]</sup> Jean-Paul Mazaleyra,<sup>[c]</sup> and Michel Wakselman<sup>[c]</sup>

**Abstract:** Two hexapeptides, each bearing one photoactive  $\alpha$ -amino acid (Bin or Bpa) and one nitroxide-containing TOAC residue, have been synthesized and fully characterized. FT-IR absorption measurements indicate that a  $3_{10}$ -helical conformation is adopted by these peptides in solution. As two amino acid units separate the photoactive residue from TOAC in the peptide sequences, the two moieties face each other at a distance of about 6 Å after one complete turn of the ternary helix. Irradiation by a

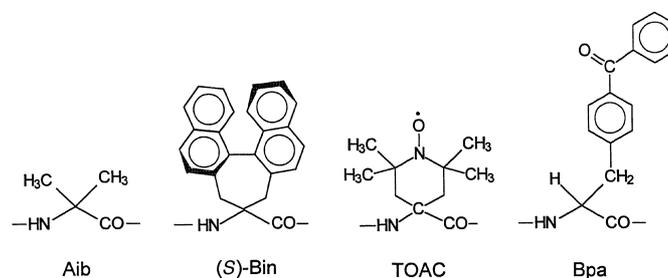
light pulse from an excimer laser populates the excited states localized on the chromophores. An intramolecular interaction between the singlet (Bin) or triplet (Bin and Bpa) excited states and the doublet state of the TOAC nitroxide makes a spin-selective decay pathway possible, that produces transient spin

polarization. In addition, in order to determine whether the intramolecular exchange interaction occurs through-bond or through-space, we have prepared linear and cyclic TOAC-Bin dipeptide units. A CIDEP study revealed that a through-space intramolecular interaction is operative. The observation of spin polarization makes the two helical hexapeptides suitable models to test the possibility of application of this novel technique to conformational studies of peptides in solution.

**Keywords:** chromophores • CIDEP • EPR spectroscopy • helical peptides • intramolecular interaction

## Introduction

The unique stereochemistry of peptides containing C $^{\alpha}$ -tetrasubstituted  $\alpha$ -amino acids,<sup>[1]</sup> that severely restrict their conformational freedom, allows for their exploitation as precise molecular rulers,<sup>[2]</sup> scaffolding blocks in the de novo design of protein and enzyme mimetics,<sup>[3]</sup> and suitable models for spectroscopic studies.<sup>[4]</sup> Aib ( $\alpha$ -aminoisobutyric acid, Figure 1), the prototype of C $^{\alpha}$ -tetrasubstituted  $\alpha$ -amino acids, is a strong helix promoter. In particular, Aib *homo*-peptides and Aib-rich, short oligopeptides adopt predominantly the  $3_{10}$ -helical conformation both in solution and in the crystal state.<sup>[1]</sup> A similar behavior was found for the two other C $^{\alpha}$ -tetrasub-



- 1 Fmoc-Aib-Ala-TOAC-Ala-Ala-OtBu
- 2 Boc-Bpa-Aib-Ala-TOAC-Ala-Ala-OtBu
- 3 Boc-(S)-Bin-Ala-Aib-TOAC-Ala-Ala-OtBu
- 4 Fmoc-TOAC-(S)-Bin-OMe
- 5 Boc-TOAC-(S)-Bin-OMe
- 6 *cyclo*[TOAC-(S)-Bin]

Figure 1. Chemical formulas of amino acids and sequences of peptides discussed in this work.

stituted  $\alpha$ -amino acids discussed in this work, the nitroxide-based TOAC (2,2,6,6-tetramethylpiperidine-1-oxyl-4-amino-4-carboxylic acid)<sup>[4a, 4c, 5]</sup> and the axially chiral, photoexcitable Bin (2',1':1,2;1'',2'':3,4-dinaphthylcyclohepta-1,3-diene-6-amino-6-carboxylic acid).<sup>[6]</sup>

The  $3_{10}$ -helix, the third principal long-range structural element occurring in globular proteins beside the  $\alpha$ -helix

[a] Prof. C. Corvaja, Dr. E. Sartori, Dr. A. Toffoletti  
Department of Physical Chemistry, University of Padova  
35131 Padova (Italy)  
Fax: (+ 39) 049 827-5135  
E-mail: corvaja@chfi.unipd.it

[b] Prof. C. Toniolo, Dr. F. Formaggio, Dr. M. Crisma  
Biopolymer Research Centre, CNR  
Department of Organic Chemistry, University of Padova  
35131 Padova (Italy)  
Fax: (+ 39) 049 827-5239  
E-mail: biop02@chor.unipd.it

[c] Dr. J.-P. Mazaleyra, Dr. M. Wakselman  
SIRCOB, Bât. Lavoisier, University of Versailles  
78000 Versailles (France)



could represent a potentially useful phenomenon to investigate the solution conformation of this class of biomolecules.

In this work we synthesized and studied terminally protected hexapeptides **2** and **3** (Figure 1), each containing a photoexcitable amino acid [(*S*)-Bpa (4'-benzoylphenylalanine) and (*S*)-Bin] and a free-radical TOAC<sup>[4a, 4c, 5, 6b, 6c, 13b-d]</sup> unit. The chromophore and TOAC, spaced by two residues, are approximately located one on top of the other when the peptides are folded in the putative ternary  $3_{10}$ -helical conformation. In **2** and **3** such an ordered secondary structure is stabilized by the presence of two and three C $^{\alpha}$ -tetrasubstituted  $\alpha$ -amino acid residues, respectively.<sup>[1]</sup> Thus, CIDEP might confirm that TOAC and the chromophore are separated by a short distance ( $\cong 6$  Å), corresponding to the pitch of the  $3_{10}$ -helix. The photoexcitable chromophore in peptide **2** is the benzophenone derivative<sup>[27]</sup> in the side chain of the phenylalanine analogue Bpa, while in peptide **3** is the binaphthyl derivative<sup>[28]</sup> characterizing the Bin residue. With the aim at investigating the role played by through-bond or through-space RS and RT interactions, we also prepared and examined the model compounds **5** and **6**, in which TOAC and Bin are directly covalently linked to form a flexible linear dipeptide and a semi-rigid cyclic dipeptide (diketopiperazine, DKP), respectively.

## Results and Discussion

**Synthesis and characterization:** TOAC<sup>[5a, 5d, 13b]</sup> and (*S*)-Bin<sup>[29]</sup> were synthesized according to published procedures. All peptides were prepared by solution methods. The synthesis and characterization of hexapeptide **3**<sup>[6c]</sup> have already been reported. Pentapeptide **1** was prepared in 90% yield from Fmoc-Aib-OH and H-Ala-TOAC-Ala-Ala-OrBu [obtained from the corresponding Fmoc N-protected tetrapeptide<sup>[4a]</sup> by treatment with a 25% (*v/v*) diethylamine solution in CH<sub>2</sub>Cl<sub>2</sub>] by employing the highly efficient EDC/HOAt [EDC, 1-(3-dimethylaminopropyl)-3-ethylcarbodiimide; HOAt, 1-hydroxy-7-azabenzotriazole] condensation method.<sup>[30]</sup> Using the same procedure, Boc-Bpa-OH was coupled to the Fmoc-deprotected peptide **1** to give **2** in 70% yield. Also in the preparation of the linear dipeptide **4**, involving the difficult coupling between Fmoc-TOAC-OH and H-(*S*)-Bin-

OMe,<sup>[29]</sup> the EDC/HOAt method gave a good result (88% yield). Fmoc-deprotection of **4** afforded H-TOAC-(*S*)-Bin-OMe which was reacted with Boc<sub>2</sub>O in CH<sub>3</sub>CN for three days at 50 °C to give the *N*-Boc protected dipeptide **5** in a moderate yield (38%). The same *N*-deprotected dipeptide was cyclized to the diketopiperazine **6** in a 73% yield by refluxing it in a toluene/acetic acid 20:1 (*v/v*) mixture for six hours.

All peptides were characterized by melting point and optical rotatory power determinations, thin-layer chromatography (TLC) in two solvent systems, molecular mass determination, and solid-state IR absorption (Table 1).

**Conformational analysis:** As the NMR technique does not provide useful structural information on free radical compounds, the conformational preferences of hexapeptides **2** and **3** in CDCl<sub>3</sub> solution were heavily based on FT-IR absorption spectroscopy. The IR absorption spectra of **2** and **3** in the informative amide A (N–H stretching) region are illustrated in Figure 2. Relevant conclusions are the following: i) The weak band centered at about 3420 cm<sup>-1</sup> is assigned to free, solvated peptide N–H groups, while the intense band at about 3330 cm<sup>-1</sup> is assigned to H-bonded peptide NH groups.<sup>[31, 32]</sup> ii) The spectra do not appreciably change in the concentration range examined (10–0.1 mM); this finding indicates that the 3330 cm<sup>-1</sup> band is essentially due to intramolecularly H-bonded peptide NH groups. iii) The high values for the  $A_H/A_F$  ratio (integrated intensity of the band of H-bonded NH groups to

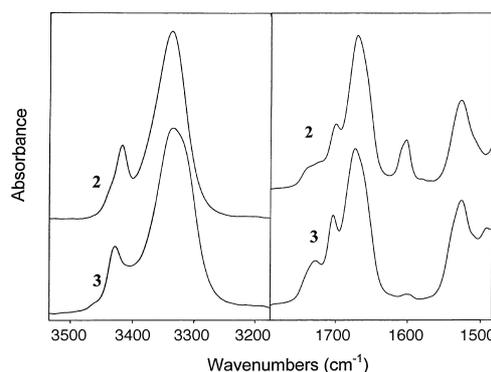


Figure 2. FT-IR absorption spectra of peptides **2** and **3** in the 3500–3200 cm<sup>-1</sup> (left) and 1800–1500 cm<sup>-1</sup> (right) spectral regions in CDCl<sub>3</sub> solution (conc. 1 mM).

Table 1. Physical properties and analytical data for peptides **1**, **2**, **4**–**6**.

Compound	M.p. [°C] <sup>[a]</sup>	Recryst. solvent <sup>[b]</sup>	[ $\alpha$ ] <sub>D</sub> <sup>20</sup> <sup>[c]</sup>	TLC <sup>[f]</sup>		IR [cm <sup>-1</sup> ] <sup>[g]</sup>	MS <sup>[h]</sup> <i>m/z</i>
				<i>R</i> <sub>f</sub> (I)	<i>R</i> <sub>f</sub> (II)		
<b>1</b>	166–168	EtOAc/PE	–24 <sup>[d]</sup>	0.95	0.45	3330, 1720, 1663, 1531	794 [ <i>M</i> +2H] <sup>+[i]</sup> , 815 [ <i>M</i> +Na] <sup>+</sup>
<b>2</b>	144–146	EtOAc/PE	2 <sup>[e]</sup>	0.95	0.30	3325, 1724, 1661, 1530	923 [ <i>M</i> +2H] <sup>+[i]</sup> , 944 [ <i>M</i> +Na] <sup>+</sup>
<b>4</b>	203–204	CH <sub>2</sub> Cl <sub>2</sub> /DE	133	0.95	0.70	3424, 3380, 1730, 1712, 1677	786 (38) [ <i>M</i> ] <sup>+</sup> , 788 (100) [ <i>M</i> +2H] <sup>+[i]</sup>
<b>5</b>	112–113	DE/PE	67	0.95	0.65	3371, 1722, 1688	666 (100) [ <i>M</i> +2H] <sup>+[i]</sup>
<b>6</b>	246–247	MeOH/DE	92	0.90	0.50	3374, 3249, 1674	532 (18) [ <i>M</i> ] <sup>+</sup> , 534 (100) [ <i>M</i> +2H] <sup>+[i]</sup>

[a] Determined on a Leitz model Laborlux 12 apparatus. [b] EtOAc, ethyl acetate; PE, petroleum ether; DE, diethyl ether. [c] Determined on a Perkin–Elmer model 241 polarimeter equipped with a Haake model L thermostat: *c* = 0.1 (MeOH). [d] *c* = 0.25 (MeOH). [e] *c* = 0.5 (MeOH). [f] Silica gel plates (60F<sub>254</sub>, Merck), using the following solvent systems: I) chloroform/ethanol 9:1; II) toluene/ethanol 7:1. The compounds were revealed either with the aid of a UV lamp or with the hypochlorite/starch/iodide chromatic reaction, as appropriate. A single spot was observed in each case. [g] Determined in KBr pellets on a Perkin–Elmer model 580 B spectrophotometer equipped with a Perkin–Elmer model 3600 IR data station and a model 660 printer. Only bands in the 3500–3200 cm<sup>-1</sup> and 1800–1500 cm<sup>-1</sup> regions are listed. [h] MALDI-TOF for compounds **1** and **2**; ES (relative intensities between round brackets) for compounds **4**–**6**. [i] Reduction to N-OH and subsequent protonation has already been reported for nitroxide containing derivatives [O. H. Hankowsky, C. P. Sár, K. Hideg, G. Jerkovich, *Synthesis* **1991**, 91–97].

free NH groups)<sup>[33]</sup> are indicative of stable helical secondary structures. In addition, in both peptides **2** and **3** the position of the absorption maximum for the amide I (C=O stretching) band is close to the values typical of  $\alpha$ - and  $3_{10}$ -helices.<sup>[10]</sup> Taken together, these observations indicate that an intramolecularly H-bonded helical structure is largely populated by hexapeptides **2** and **3** in CDCl<sub>3</sub> solution. In view of their short main-chain length it is plausible to assume that the type of helix adopted by **2** and **3** would be the  $3_{10}$ -helix.<sup>[1b]</sup>

This conclusion matches well with the results of the recent X-ray diffraction structure determination of **3** in the crystal state.<sup>[6b, 6c]</sup> The  $-(S)\text{-Bin}^1\text{-Ala-Aib-TOAC}^4\text{-}$  sequence of both independent molecules in the asymmetric unit of the hexapeptide is folded in a regular, left-handed  $3_{10}$ -helix, stabilized by three consecutive  $i \leftarrow i + 3$  C=O...H-N intramolecular H-bonds. In both molecules the distance between the C $^{\alpha}$  atoms of Bin<sup>1</sup> and TOAC<sup>4</sup>, after one complete turn of the  $3_{10}$ -helix, is close to 5.8 Å.

**EPR measurements:** The relevant photophysical properties of the 1,1-binaphthyl and benzophenone chromophores are listed in Table 2. Laser light at  $\lambda = 308$  nm is absorbed by both benzophenone and binaphthyl, whereas absorption of TOAC at this wavelength is negligible. Benzophenone has a short-lived excited singlet state which converts in ps time scale into a triplet state with a practically unity yield. The fluorescence yield is almost zero. Conversely, the lifetime of the excited singlet state of Bin is few ns and the fluorescence yield is large. No data are available for triplet yield and energy. However, their values are likely to be close to those of naphthalene.

Figure 3 shows the cw-EPR spectrum of **2** in CHCl<sub>3</sub> recorded at  $T = 260$  K. The spectrum appears as the first derivative of the absorption since the usual 100 kHz field modulation and lock-in detection were used. It consists of three narrow lines (linewidth 1.0–1.5 Gauss), separated by  $a_N = 15.65$  G, due to the hyperfine interaction of the TOAC unpaired electron with the <sup>14</sup>N nucleus of the nitroxide group. <sup>13</sup>C satellite lines are also visible. The small linewidth indicates that in this solvent **2** is not self-aggregated. This finding agrees well with the results extracted from the FT-IR absorption analysis performed in the same solvent (see above).

Figure 4a shows the EPR signal of peptide **2** in CHCl<sub>3</sub> solution evoked by a laser pulse ( $\lambda = 308$  nm) as a surface in magnetic field and time coordinates (2D-TR-EPR spectrum).<sup>[34]</sup> The signal was recorded by direct detection without magnetic field modulation. The negative EPR signal is

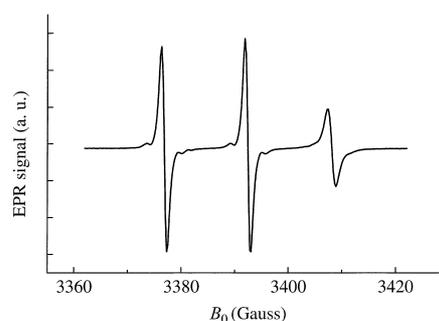


Figure 3. cw-EPR spectrum of peptide **2** in CHCl<sub>3</sub> solution (conc. 10 mM) at 260 K.

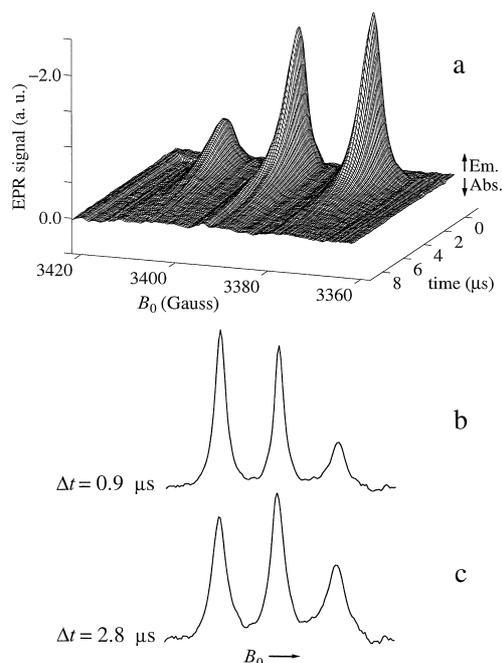


Figure 4. a) 2D-TR-EPR spectrum of peptide **2** in CHCl<sub>3</sub> solution (conc. 10 mM) at 260 K; b) and c) are sections of the 2D spectrum at  $\Delta t = 0.9 \mu\text{s}$  and  $2.8 \mu\text{s}$ .  $\Delta t$  is the delay time after the laser pulse.

associated with true emission. The sections of the surface (Figures 4b and 4c) parallel to the magnetic field axis, representing the spin polarized EPR spectrum at a fixed delay after the laser pulse, are simulated by three Lorentzian lines having different widths and intensities. The intensity ratios between the lines change considerably with the delay time  $\Delta t$  after the laser shot, because of a different time evolution of the three lines. At short delay times ( $\Delta t < 1.3 \mu\text{s}$ )

Table 2. Photophysical properties of the chromophores.<sup>[a]</sup>

Compound	Solvent	$\lambda_s^{0-0[b]}$ (nm)	$\epsilon(\lambda = 308 \text{ nm})$ ( $\text{l mol}^{-1} \text{ cm}^{-1}$ )	$\tau_s^{[c]}$ (ns)	$\Phi_f^{[d]}$	$E_T^{[e]}$ ( $\text{cm}^{-1}$ )	$\tau_T^{[c]}$ ( $\mu\text{s}$ )	$\Phi_T^{[d]}$
Benzophenone	apolar	379	$\approx 40$	0.030	$4 \times 10^{-6}$	24000	6.9	1.0
	polar	384	$\approx 110$	0.016		24200	50	1.0
1,1'-Binaphthyl	apolar	325	$\approx 5000$	3.0	0.77		14	
	polar	328						
Naphthalene	apolar	311	$\approx 110$	96	0.19	21180	175	0.75
	polar	311	$\approx 100$	105	0.21	21300	1800	0.80

[a] Taken from: S. L. Murov, I. Carmichael, G. L. Hug, *Handbook of Photochemistry*, Dekker, New York, 1993. [b]  $\lambda_s^{0-0}$ , wavelength of the transition between the 0 vibrational levels of the fundamental and excited singlet states. [c]  $\tau_s$  and  $\tau_T$ , excited singlet and triplet lifetimes. [d]  $\Phi_f$ , fluorescence quantum yield;  $\Phi_T$ , triplet quantum yield. [e]  $E_T$ , triplet excited state energy.

the intensity of the hyperfine components decreases from low field to high field; this indicates that the nitrogen nucleus hyperfine interaction contributes to the polarization mechanism. At longer delay times the central line appears as the most intense. Figure 5 shows the sections of the surface parallel to the time axis, at the field values corresponding to the maximum intensity of each line. The time evolution of the lines is perfectly fit by a two-exponential function. The fitting curves, obtained with the parameters listed in Table 3, are also shown.

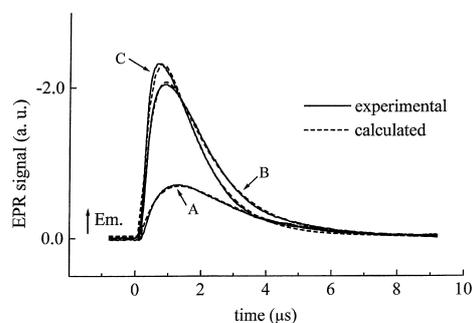


Figure 5. Sections of the surface parallel to the time axis in Figure 4 and their fittings. **A**, high-field line; **B**, central line; **C**, low-field line.

Table 3. Experimentally determined time constants for the individual components of the TR-EPR spectra.

Peptide		Time constants ( $\mu\text{s}$ )		
		B: low field	C: central field	A: high field
<b>2</b>	$\tau_1$	0.4	0.4	0.9
	$\tau_2$	1.2	1.4	1.5
<b>3</b>	$\tau_0$	< 0.2	< 0.2	< 0.2
	$\tau_1$	0.5	0.6	0.8
	$\tau_2$	2.7	3.1	4.5

We attribute the strong spin polarization in emission of the nitroxide EPR lines to an interaction between the triplet benzophenone moiety and the TOAC radical according to the radical triplet pair mechanism (RTPM).<sup>[18]</sup> For the Bpa-containing peptide **2** only triplet quenching has to be considered, because triplet formation by ISC due to spin-orbit coupling (SOC) is a very fast and efficient process. The observed polarization is very large if compared with the case of separated benzophenone and nitroxide at similar concentrations.<sup>[18b, 19]</sup> This finding strongly points to an intramolecular interaction. Further evidence, based on the results obtained for **5** and **6**, will be discussed later.

To our knowledge, this is the first time that the contribution of the hyperfine interaction to the intramolecular RTPM is observed. It is reasonable to assume that the occurrence of the intramolecular RT interaction would be favored by the  $3_{10}$ -helical structure of the peptide, which brings the partners about 6–7 Å close to each other.

Similar results were obtained for peptide **3** (Figure 6). The 2D-TR-EPR spectrum shows a strong three-line spin polarized signal in which the intensity ratios among the lines are due to a contribution of the hyperfine interaction to the polarization mechanism. However, at variance with the previous case, the initial spin polarization is in enhanced

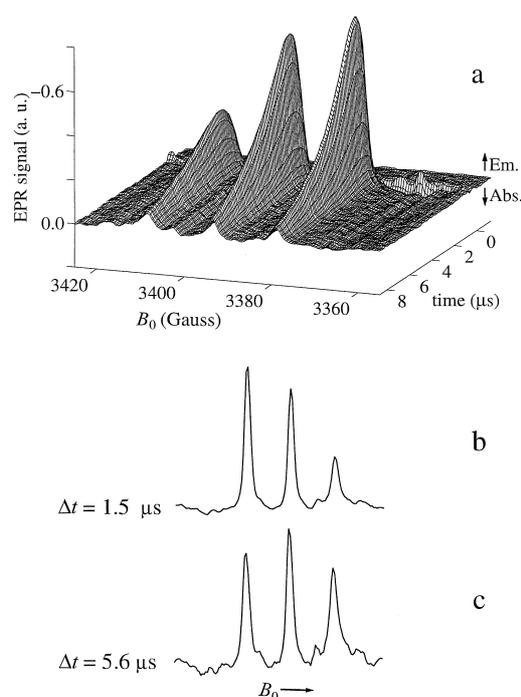


Figure 6. a) 2D-TR-EPR spectrum of peptide **3** in  $\text{CH}_3\text{CN}$  solution (conc. 10 mM) at 260 K; b) and c) are sections of the 2D spectrum at  $\Delta t = 1.5 \mu\text{s}$  and  $5.6 \mu\text{s}$ .  $\Delta t$  is the delay time after the laser pulse.

absorption (Figure 7). Only at later times the enhanced absorption signal reverts into emission and eventually becomes zero. The time evolution of the signal is simulated by a three-exponential function. Unfortunately, the fastest decay rate ( $\tau_0$  in Table 3) cannot be determined with precision since

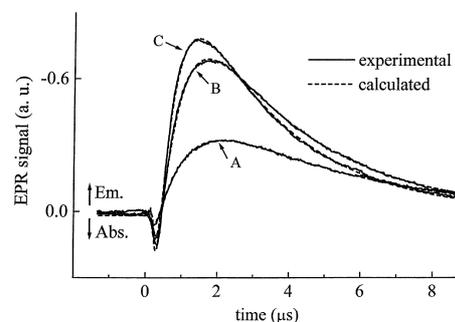


Figure 7. Sections of the surface parallel to the time axis in Figure 6 and their fittings. **A**, high-field line; **B**, central line; **C**, low-field line.

the signal changes too fast compared with the time resolution of our experimental setup, which is of the order of 200 ns. Spectra recorded with a boxcar integrator, using an integration window placed at short delay time, unequivocally confirm the initial character of the spectrum in enhanced absorption. We therefore exclude that the initial signal in absorption would be an instrumental artefact because repeated TR-EPR experiments have shown this feature for Bin-containing peptides **3** and **6**, but not for the Bpa-containing peptide **2** and several other systems studied in this laboratory with the same setup.

In a RT pair the exchange energy  $J$  is expected to be negative, with the exception of particular cases.<sup>[15]</sup> For a

negative exchange interaction  $J$  an EPR spectrum in enhanced absorption is expected when singlet quenching takes place, whereas the spectrum is in emission when triplet quenching occurs. For **2** only triplet quenching occurs, while the pattern shown in the EPR signal of **3** indicates that both singlet and triplet quenchings take place for Bin. Indeed, Bin, in contrast to Bpa, has an excited singlet state with a long enough life. These findings demonstrate that for both peptides **2** and **3**  $J$  is negative. It is noteworthy that a similar polarization pattern (first in enhanced absorption and then in emission) has been already observed in TR-EPR spectra arising from intermolecular interactions of TEMPO radicals with photoexcited naphthalene molecules,<sup>[19]</sup> which excited state properties are similar to those of Bin.

Recently, some of us have observed that the fluorescence of Bin in **3** is quenched by TOAC.<sup>[6b, 6c]</sup> In addition, the excited-state lifetime is shortened as compared with that of Boc-(S)-Bin-OrBu. Quenching was explained in terms of an energy transfer mechanism. Our present observation of initial polarization in enhanced absorption indicates that Bin singlet quenching should take place, at least in part, through electron exchange-induced intersystem crossing to the triplet state.

In order to assess whether the exchange interaction occurs through-bond or through-space we have designed and synthesized dipeptides **5** and **6**, where the nitroxide group and the Bin  $\pi$ -system are separated by eight bonds only, instead of fourteen bonds as in peptides **2** and **3**. Dipeptides **5** and **6** differ in the overall molecular flexibility, as **5** is a relatively flexible, linear compound, whereas **6** is a backbone-cyclized, semi-rigid molecule. While in the case of the linear dipeptide **5** no signal was recorded after laser irradiation, in the case of the cyclic dipeptide **6** a strong TR-EPR signal was noted, having the same characteristics as those exhibited by hexapeptide **3** (Figure 6). The intriguing observation that **5** does not give rise to a spin-polarized spectrum, while **6** does, strongly supports the view that a through-bond interaction is not operative, since in the two dipeptides the radical and the chromophore are separated by the same number of covalent bonds. Moreover, if the RT interaction takes place between different molecules, we would expect the same behavior for **5** and **6**. This result confirms that an intramolecular interaction is taking place.

As for the different initial emission intensity of the individual hyperfine lines of both **2** and **3**, it is worth reminding that any spin polarized spectrum can be considered as a combination of a spectrum due to net effect and a spectrum due to multiplet effect, that occurs when CIDEP is generated by the hyperfine interaction.<sup>[16]</sup> According to the RTPM, which is appropriate in our case, spin polarization is produced because of the mixing of the doublet and quartet states of the RT pair, due to both the electron–electron dipolar interaction between the triplet unpaired electrons and the electron–nucleus hyperfine interaction.<sup>[18b]</sup> For triplet quenching, the former type of interaction gives rise to a net emission (or to an enhanced absorption, if  $J > 0$ ), while the latter type of interaction gives emission for the low-field component, absorption for the high-field component, and zero polarization for the central component (or viceversa depending upon the sign of the product  $J \cdot a_N$ <sup>[18b]</sup>).

According to the proposed model for RTPM, the magnitude of net polarization is expected to reach a maximum at the crossings of the  $D_{-1/2}$  level with  $Q_{+3/2}$  and  $Q_{+1/2}$  levels. These crossings are seen for  $J_1 = -(2/3)g\beta B$  and  $J_2 = -(1/3)g\beta B$ , corresponding to well defined distances  $r_1$  and  $r_2$  between the radical and triplet molecules. An exponential dependence of  $J$  from distance is usually assumed:

$$J = J_0 \exp(-\lambda(r-d)).$$

However, the values assigned to the parameters are not univocal.<sup>[35]</sup> By taking the set  $\lambda = 1.4 \text{ \AA}^{-1}$ ,  $J_0 = 1.5 \times 10^{10} \text{ Hz}$ , and  $d = 7 \text{ \AA}$ , the values  $r_1 = 7.6 \text{ \AA}$  and  $r_2 = 8.1 \text{ \AA}$  were obtained.<sup>[35a]</sup> These values are close to the TOAC...chromophore distance for the peptide in a helical conformation (the averaged intramolecular distance between the nitroxyl nitrogen atom of TOAC and the center of the two naphthyl units of Bin for **3** in the crystal state is  $6.22 \text{ \AA}$  for molecule **A** and  $6.59 \text{ \AA}$  for molecule **B**).<sup>[6b, 6c]</sup> For a complete unfolded conformation this distance would be of the order of  $15 \text{ \AA}$  and the corresponding calculated value  $J = 2 \times 10^5 \text{ Hz}$ . For this value of  $J$  we should observe only a multiplet effect, which occurs when the doublet and quartet states are almost degenerate, while we noted a predominant net polarization. At present, the lack of reliable information on the dependence of the exchange interaction on the radical–triplet distance does not allow an accurate measurement to be performed. However, it is evident that in our systems the observed polarization can occur only if the peptide is in the helical form.

Concerning the different time evolution of the polarization of the individual EPR lines, we attribute it to the effect of Heisenberg spin exchange.

For a spin  $S = 1/2$  stable free radical containing a  $I = 1$  nuclear spin, in a magnetic field, there are six energy levels, characterized by  $\alpha$  and  $\beta$  (the electron spin components) and by the nuclear spin components  $0, \pm 1$ . The concentrations ( $n$ ) of free radicals in the individual levels change with time according to the solution of a system of differential equations, which takes into account the spin relaxation, the Heisenberg electron spin exchange, and the polarization source. The three equations for the  $\alpha$  sublevels have the following form:

$$\begin{aligned} \frac{dn_i^\alpha}{dt} = & -w(n_i^\alpha - n_i^\beta - k_{\text{ex}}n_i^\alpha(n_j^\beta + n_k^\beta) - k_{\text{ex}}n_i^\beta(n_j^\alpha + n_k^\alpha) \\ & + n_s(k_{\text{net}} + k_{\text{mul}}\delta_{1,i} - k_{\text{mul}}\delta_{-1,i})) \end{aligned} \quad (1)$$

where the indexes  $i, j$ , and  $k$  indicate different nuclear spin components,  $w$  is the rate constant including the relaxation and the microwaves effect, and  $k_{\text{ex}}$  is the Heisenberg exchange rate constant. In the last term, which accounts for the initial polarization,  $n_s$  is the concentration of a fictitious level acting as source,  $k_{\text{net}}$  is the rate constant of the populating process producing net effect, and  $k_{\text{mul}}$  is the rate constant of the populating process producing multiplet effect.

Three analogous equations for the  $\beta$  sublevels can be written by exchanging throughout  $\alpha$  with  $\beta$  and neglecting the source term in Equation (1). A seventh differential equation for the fictitious level has to be included in the system.

Heisenberg spin exchange affects the line polarization only if there is a multiplet effect. In the case of the three-line

spectrum of the nitroxide radical, polarization is transferred from the low-field line to the high-field one, while the central line is not modified. Solutions to the differential equations relevant to this latter line depend only on  $w$  and  $k_{\text{net}}$ , which can be obtained with a best fit procedure that gives for peptide **2** the values  $w = 2.85 \times 10^5 \text{ s}^{-1}$  and  $k_{\text{net}} = 1.5 \times 10^6 \text{ s}^{-1}$ . For a qualitative description of the time evolution of the other two lines, different populating rates ( $k_{\text{net}} \pm k_{\text{mul}}$ , with  $k_{\text{mul}} \cong 1 \times 10^6 \text{ s}^{-1}$ ) should be assumed. Moreover, addition of the Heisenberg spin exchange term is necessary.

A quantitative determination would require knowledge of the Boltzmann equilibrium signal intensity, which cannot be obtained from our experiments. Indeed, in contrast to the case of CIDEP of transient species, the TR-EPR signal of stable radicals measures the EPR signal variation with respect to a zero level which corresponds to Boltzmann equilibrium. Furthermore, even if the equilibrium polarization might be calculated from Curie's law, it would be necessary to know the initial concentration of triplet species. However, this information is not available owing to the geometry of our experimental setup. Specifically, due to the limited amounts of peptides available and the polarity of the solvents, the samples are placed in a 1-mm inner diameter cylindrical tube, which is inserted in a quartz Dewar and irradiated from the outside. The estimated number of photons actually absorbed by the solution is affected by an error too large to be exploited for an accurate determination of the initial concentration of triplets. If we assume that the fraction of excited molecules immediately after the laser pulse would be 0.01, then a value of  $k_{\text{ex}} = 100 \text{ MHz l mol}^{-1}$  fits the experimental data. This exchange rate is not large enough to affect the lineshape of the cw-EPR spectrum.

## Conclusion

In all four Bpa/TOAC and Bin/TOAC peptides examined in this work and giving transient EPR spectra, TOAC intramolecularly quenches their triplet state by enhanced ISC to the ground state via an electron-exchange process. Moreover, in the Bin/TOAC peptides **3** and **6** the electron-exchange interaction quenches the singlet excited state as well. Quenching of Bin fluorescence by TOAC has been recently attributed to an energy transfer process.<sup>[6b, 6c]</sup> At this stage, it is difficult to discriminate whether this latter mechanism or the enhanced ISC is the main pathway for singlet decay. In any case, this work unambiguously demonstrates that enhanced ISC does occur.

By investigating two appropriately designed Bin/TOAC models we have also been able to show that the intramolecular electron-exchange process takes place through space. This finding strongly suggests that CIDEP can be exploited as a novel method for the analysis of peptide secondary structures in solution. To check this proposal in more detail, we are currently comparing the CIDEP effects of conformationally well-characterized helical peptides with the photoactive Bpa or Bin and free-radical TOAC units located at different relative backbone positions.

## Experimental Section

**Materials:** Bpa was obtained from Bachem (Switzerland). The physical properties and the analytical data for peptides **1**, **2**, **4–6** are listed in Table 1.

**FT-IR absorption:** FT-IR absorption spectra were recorded with a Perkin–Elmer model 1720X spectrophotometer, nitrogen flushed, equipped with a sample-shuttle device, at  $2 \text{ cm}^{-1}$  nominal resolution, averaging 100 scans. Solvent (base-line) spectra were recorded under the same conditions. Cells with path lengths of 0.1, 1.0 and 10 mm (with  $\text{CaF}_2$  windows) were used. Spectrograde  $[\text{H}]\text{CHCl}_3$  (99.8%  $^2\text{H}$ ) was purchased from Fluka.

**EPR measurements:** Peptide solutions of about  $1 \times 10^{-2} \text{ M}$  concentration in  $\text{CH}_3\text{CN}$  (Fluka),  $\text{CHCl}_3$  (Prolabo) and toluene (Prolabo) were prepared directly in the EPR quartz tubes (o.d. = 2 or 3 mm) and carefully deoxygenated by bubbling nitrogen gas. The solvents were used as purchased, without any further purification. EPR spectra were recorded on a cw EPR spectrometer (Bruker ER 200 D) operating in the X band and equipped with a liquid nitrogen cryostat. Time-resolved EPR measurements were performed by collecting the signal from the microwave detector with a 400 MHz digital oscilloscope (LeCroy 9450A) without using the 100 kHz field modulation. Photoexcitation was achieved by irradiating the samples, inside the cavity of the spectrometer, with 20 ns light pulses from an excimer XeCl laser (Lambda Physik LPX 100, = 308 nm). The light was directed on the sample by means of a quartz optic fibre (quartz diameter = 1 mm). Field-time two-dimensional surfaces were obtained in the following way: one transient EPR signal was recorded at a fixed field position, averaged (200–400 times), and stored in a PC. Then, the field was incremented and the process repeated for 128 different field positions. An in-house written software was used to control the field steps and data acquisition.

## Acknowledgement

The authors wish to thank Milena Bressanini for her contribution to the synthesis of peptides **4–6** and the National Research Council (C.N.R.) and Ministry of University and Scientific and Technological Research (M.U.R.S.T.) of Italy for the continuous financial support.

- [1] a) B. V. Venkataram Prasad, P. Balaram, *CRC Crit. Rev. Biochem.* **1984**, *16*, 307–348; b) I. L. Karle, P. Balaram, *Biochemistry* **1990**, *29*, 6747–6756; c) C. Toniolo, E. Benedetti, *Macromolecules* **1991**, *24*, 4004–4009; d) C. Toniolo, M. Crisma, F. Formaggio, G. Valle, G. Cavicchioni, G. Précigoux, A. Aubry, J. Kamphuis, *Biopolymers* **1993**, *33*, 1061–1072.
- [2] A. Polese, F. Formaggio, M. Crisma, G. Valle, C. Toniolo, G. M. Bonora, Q. B. Broxterman, J. Kamphuis, *Chem. Eur. J.* **1996**, *2*, 1104–1111.
- [3] a) R. Kaul, *Bioorg. Med. Chem.* **1999**, *7*, 105–117; b) P. Rossi, F. Felluga, P. Tecilla, F. Formaggio, M. Crisma, C. Toniolo, P. Scrimin, *J. Am. Chem. Soc.* **1999**, *121*, 6948–6949.
- [4] a) P. Hanson, G. Millhauser, F. Formaggio, M. Crisma, C. Toniolo, *J. Am. Chem. Soc.* **1996**, *118*, 7618–7625; b) R. Gratias, R. Konat, H. Kessler, M. Crisma, G. Valle, A. Polese, F. Formaggio, C. Toniolo, Q. B. Broxterman, J. Kamphuis, *J. Am. Chem. Soc.* **1998**, *120*, 4763–4770; c) B. Pispisa, L. Stella, M. Venanzi, A. Palleschi, F. Marchiori, A. Polese, C. Toniolo, *Biopolymers* **2000**, *53*, 169–181.
- [5] a) C. Toniolo, E. Valente, F. Formaggio, M. Crisma, G. Piloni, C. Corvaja, A. Toffoletti, G. V. Martinez, M. P. Hanson, G. L. Millhauser, C. George, J. L. Flippen-Anderson, *J. Pept. Sci.* **1995**, *1*, 45–57; b) J. L. Flippen-Anderson, C. George, G. Valle, E. Valente, A. Bianco, F. Formaggio, M. Crisma, C. Toniolo, *Int. J. Pept. Protein Res.* **1996**, *47*, 231–238; c) M. Crisma, V. Monaco, F. Formaggio, C. Toniolo, C. George, J. L. Flippen-Anderson, *Lett. Pept. Sci.* **1997**, *4*, 213–218; d) C. Toniolo, M. Crisma, F. Formaggio, *Biopolymers (Pept. Sci.)* **1998**, *47*, 153–158.
- [6] a) J.-P. Mazaleyat, A. Gaucher, M. Wakselman, C. Toniolo, M. Crisma, F. Formaggio in *Peptides 1996* (Eds.: R. Ramage, R. Epton), Mayflower, Kingswinford, England, **1998**, pp. 623–624; b) C. Toniolo, F. Formaggio, M. Crisma, J.-P. Mazaleyat, M. Wakselman, C. George,

- J. L. Flippen-Anderson, B. Pispisa, M. Venanzi, A. Palleschi in *Peptides: Frontiers of Peptide Science* (Eds.: J. P. Tam, P. T. P. Kaumaya), Kluwer, Dordrecht, The Netherlands, **1999**, pp. 378–380;
- c) C. Toniolo, F. Formaggio, M. Crisma, J.-P. Mazaleyrat, M. Wakselman, C. George, J. R. Deschamps, J. L. Flippen-Anderson, B. Pispisa, M. Venanzi, A. Palleschi, *Chem. Eur. J.* **1999**, *5*, 2254–2264.
- [7] D. J. Barlow, J. M. Thornton, *J. Mol. Biol.* **1988**, *201*, 601–619.
- [8] C. Toniolo, E. Benedetti, *Trends Biochem. Sci.* **1991**, *16*, 350–353.
- [9] a) G. Basu, A. Kuki, *Biopolymers* **1993**, *33*, 995–1000; b) G. L. Millhauser, C. J. Stenland, P. Hanson, K. A. Bolin, F. J. M. van de Ven, *J. Mol. Biol.* **1997**, *267*, 963–974.
- [10] D. F. Kennedy, M. Crisma, C. Toniolo, D. Chapman, *Biochemistry* **1991**, *30*, 6541–6548.
- [11] C. Toniolo, A. Polese, F. Formaggio, M. Crisma, J. Kamphuis, *J. Am. Chem. Soc.* **1996**, *118*, 2744–2745.
- [12] a) S. C. Yasui, T. A. Keiderling, G. M. Bonora, C. Toniolo, *Biopolymers* **1986**, *25*, 79–89; b) S. C. Yasui, T. A. Keiderling, F. Formaggio, G. M. Bonora, C. Toniolo, *J. Am. Chem. Soc.* **1986**, *108*, 4988–4993; c) G. Yoder, T. A. Keiderling, F. Formaggio, M. Crisma, C. Toniolo, *Biopolymers* **1995**, *35*, 103–111.
- [13] a) S. M. Miick, G. V. Martinez, W. R. Fiori, A. P. Todd, G. L. Millhauser, *Nature* **1992**, *359*, 653–655; b) M. L. Smythe, C. R. Nakaie, G. R. Marshall, *J. Am. Chem. Soc.* **1995**, *117*, 10555–10562; c) P. Hanson, G. Martinez, G. Millhauser, F. Formaggio, M. Crisma, C. Toniolo, C. Vita, *J. Am. Chem. Soc.* **1996**, *118*, 271–272; d) P. Hanson, D. J. Anderson, G. Martinez, G. Millhauser, F. Formaggio, M. Crisma, C. Toniolo, C. Vita, *Mol. Phys.* **1998**, *95*, 957–966.
- [14] a) M. Crisma, A. Bianco, F. Formaggio, C. Toniolo, J. Kamphuis, *Lett. Pept. Sci.* **1995**, *2*, 187–189; b) M. Crisma, A. Bianco, F. Formaggio, C. Toniolo, C. George, J. L. Flippen-Anderson in *Recent Advances in Tryptophan Research: Tryptophan and Serotonin Pathways* (Eds.: G. Allegri Filippini, C. V. L. Costa, A. Bertazzo), Plenum Press, New York, **1996**, pp. 623–626.
- [15] a) K. M. Salikhov, Y. N. Molin, R. Z. Sagdeev, A. L. Buchachenko in *Spin Polarization and Magnetic Effects in Radical Reactions* (Ed.: Y. Molin), Elsevier, Amsterdam, **1984**, p. 324; b) N. Hirota, S. Yamauchi in *Dynamic Spin Chemistry* (Eds.: S. Nagakura, H. Hayashi, T. Azumi), Wiley, New York, **1998**, pp. 187–248.
- [16] *Chemically Induced Magnetic Polarization* (Eds.: L. T. Muus, P. W. Atkins, K. A. Mc Lauchlan, J. B. Pedersen), Reidel, Dordrecht, The Netherlands, **1977**.
- [17] a) S. K. Wong, J. K. S. Wan, *J. Am. Chem. Soc.* **1972**, *94*, 7197–7198; b) S. K. Wong, D. A. Hutchinson, J. K. S. Wan, *J. Chem. Phys.* **1973**, *58*, 985–989.
- [18] a) C. Blättler, F. Jent, H. Paul, *Chem. Phys. Lett.* **1990**, *166*, 375–380; b) A. Kawai, T. Okutsu, K. Obi, *J. Phys. Chem.* **1991**, *95*, 9130–9134; c) A. Kawai, K. Obi, *J. Phys. Chem.* **1992**, *96*, 5701–5704.
- [19] A. Kawai, K. Obi, *J. Phys. Chem.* **1992**, *96*, 52–56.
- [20] J. B. Birks, *Photophysics of Aromatic Molecules*, Wiley, New York, **1970**.
- [21] J. A. Green, L. A. Singer, J. H. Parks, *J. Chem. Phys.* **1973**, *58*, 2690–2695.
- [22] a) T. Förster, *Discuss. Faraday Soc.* **1959**, *27*, 7–17; b) D. L. Dexter, *J. Chem. Phys.* **1953**, *21*, 836–850.
- [23] Y. Kobori, A. Kawai, K. Obi, *J. Phys. Chem.* **1994**, *98*, 6425–6429.
- [24] C. Corvaja, M. Maggini, M. Prato, G. Scorrano, M. Venzin, *J. Am. Chem. Soc.* **1995**, *117*, 8857–8858.
- [25] K. Ishi, J. Fujisawa, Y. Ohba, S. Yamauchi, *J. Am. Chem. Soc.* **1996**, *118*, 13079–13080.
- [26] a) C. Corvaja, M. Maggini, M. Ruzzi, G. Scorrano, A. Toffoletti, *Appl. Magn. Reson.* **1997**, *12*, 477–493; b) J. Fujisawa, K. Ishi, Y. Ohba, S. Yamauchi, M. Fuhs, K. Moebius, *J. Phys. Chem.* **1997**, *A101*, 5869–5876.
- [27] a) J. C. Kauer, S. Erickson-Viitanen, H. R. J. Wolfe, W. F. DeGrado, *J. Biol. Chem.* **1986**, *261*, 10695–10703; b) G. Dormàn, G. D. Prestwich, *Biochemistry* **1994**, *33*, 5661–5673.
- [28] B. Juskowiak, *Anal. Chim. Acta* **1996**, *320*, 115–124.
- [29] J.-P. Mazaleyrat, A. Boutboul, Y. Lebars, A. Gaucher, M. Wakselman, *Tetrahedron: Asymmetry* **1997**, *8*, 619–631.
- [30] L. A. Carpino, *J. Am. Chem. Soc.* **1993**, *115*, 4397–4398.
- [31] M. Palumbo, S. Da Rin, G. M. Bonora, C. Toniolo, *Makromol. Chem.* **1976**, *177*, 1477–1492.
- [32] S. Mizushima, T. Shimanouchi, M. Tsuboi, R. Souda, *J. Am. Chem. Soc.* **1952**, *74*, 270–271.
- [33] C. Toniolo, G. M. Bonora, V. Barone, A. Bavoso, E. Benedetti, B. Di Blasio, P. Grimaldi, F. Lelj, V. Pavone, C. Pedone, *Macromolecules* **1985**, *18*, 895–902.
- [34] The same experiment, carried out also in a CH<sub>3</sub>CN solution of peptide **2**, gave similar results.
- [35] a) Y. Kobori, K. Takeda, K. Tsuji, A. Kawai, K. Obi, *J. Phys. Chem.* **1998**, *A102*, 5160–5170; b) G.-H. Goudsmit, H. Paul, A. I. Shushin, *J. Phys. Chem.* **1993**, *97*, 13243–13249.

Received: October 12, 1999

Revised version: February 2, 2000 [F2085]